Electronic and magnetic structure of ultrathin cobalt-chromium superlattices

F. Herman and P. Lambin*
IBM Research Laboratory, San Jose, California 95193

O. Jepsen
Max-Planck-Institut für Festkörperforschung, D-7000 Stuttgart 80, West Germany
(Received 26 October 1984)

In order to study exchange coupling and spin distributions at atomically abrupt ferromagnetic/antiferromagnetic interfaces, we construct lattice-matched Co/Cr superlattice models. We consider in some detail strained-layer superlattices composed of alternating regions of ferromagnetic bcc Co and antiferromagnetic bcc Cr with repeat periods ranging from 4 to 8 atomic layers. For computational simplicity, Cr is represented by a theoretically stabilized commensurate antiferromagnetic spin arrangement. The superlattice spin distributions are determined by carrying out first-principles self-consistent spin-polarized linearized muffin-tin-orbital electronic-structure calculations. We find that the magnetic properties of the Co/Cr superlattices are dominated by the ferromagnetic Co layers, though the antiferromagnetic character of bcc Cr is still evident. For superlattices containing 1 Co layer and 3 to 7 Cr layers per repeat period, there is only one stable spin arrangement corresponding to ferromagnetic coupling across the Co/Cr interfaces. For superlattices containing thicker Co regions, e.g., 3 Co layers and 5 Cr layers, there are two distinct spin arrangements corresponding to ferromagnetic as well as antiferromagnetic coupling across the Co/Cr interfaces. We also discuss lattice-matched 10-layer hcp-Co/bcc-Cr superlattices, as well as the implications of our results for other complicated Co/Cr superlattices.

I. INTRODUCTION

Progress over the past decade in the controlled growth of thin films[1,2] and compositionally modulated structures[2,3] has resulted in the synthesis of many novel materials. Among artificially layered metallic systems, magnetic overlayers on nonmagnetic substrates[4] and magnetic/nonmagnetic multilayers[5] have received the most attention. In this paper we consider another class of synthetic metals, namely, superlattices composed of ultrathin slabs of ferromagnetic Co and antiferromagnetic Cr.

These hypothetical structures provide a convenient theoretical model for studying exchange coupling and spin distributions at ferromagnetic/antiferromagnetic (F/AF) interfaces. In contrast to recent phenomenological studies of magnetic proximity effects in multilayers having macroscopic dimensions,[6] we will study Co/Cr superlattices having repeat periods ranging from 4 to 10 atomic layers, treating these within the framework of itinerant electron theory. By carrying out first-principles self-consistent spin-polarized electronic structure calculations, we determine the spatial distribution of spin magnetic moments on an atomic scale.

We are interested in elucidating the electronic and magnetic structure of F/AF interfaces as a step toward calculating the exchange or unidirectional anisotropy[7] of F/AF bilayers from a fundamental point of view. Before being able to treat exchange anisotropy in multilayers, which is of interest both scientifically[8] and technologically,[9] we will have to extend the present theoretical model so that it takes magnetocrystalline anisotropy into account. Work along these lines is in progress but lies outside the scope of the present paper.

In principle, we would like to treat systems of experimental interest, such as F/AF bilayers composed of ferromagnetic Permalloy ($Ni_{75}Fe_{25}$) and antiferromagnetic $Mn_{50}Fe_{50}$ alloy, with individual layer thicknesses ranging from 100 to 1000 Å. The magnetic properties of such F/AF bilayers are currently being investigated.[10] In practice, we cannot treat macroscopic, structurally disordered, F/AF slabs by first-principles methods. But we can make significant progress nevertheless by introducing suitable simplifying assumptions, as we demonstrated in a recent paper.[11] Instead of treating bilayers, we considered periodic structures—superlattices—so that we could take advantage of existing band-theoretical methods.

Now, in both Permalloy and MnFe alloy, the atoms are arranged at random on fcc lattices. To avoid severe computational problems arising from structural disorder, we represented these alloys by stoichiometrically equivalent, crystallographically compatible, ordered compounds, namely, Ni_3Fe (Cu_3Au structure) and MnFe (rocksalt structure). Since the lattice constants of these two compounds are nearly identical, we could construct a strained-layer superlattice having a suitably averaged lattice constant. To reduce the computational effort to a reasonable level, we restricted our attention to superlattices having repeat periods of 4 layers, with 2 atoms per layer. A noteworthy feature of this model is that the magnetic properties of the ordered compounds are nearly identical to those of their alloy counterparts, so that conclusions drawn from the ordered-compound model can be applied to structurally disordered multilayers.[11]

There is an inherent limitation, however, to using compounds as constituents. For example, with as few as 4 layers per repeat period, it is possible to construct three structurally distinct [001] superlattices, each having two layers of Ni_3Fe and two layers of MnFe, with 2 atoms in each layer. In order to understand the magnetic properties of the Ni_3Fe/MnFe system, it is necessary to carry out detailed calculations for all three structures, and then take a suitable average. As the number of atoms per repeat period increases—for a fixed stoichiometry—the number of structurally distinct superlattices increases rapidly. For the 4-layer model just described, the threefold structural multiplicity is more an annoyance than an obstacle, but for much larger supercells the structural multiplicity would pose a major computational problem.

For the present, we are more interested in developing a realistic but tractable model of F/AF interfaces than in determining the properties of a particular system. Accordingly, we will bypass the structural multiplicity problem by using elements, rather than compounds as the constituent materials. The essential challenge is finding a suitable pair of F/AF elements. After examining several possibilities, we decided to use Co and Cr because these are, respectively, ferromagnetic and antiferromagnetic in bulk, and because it is relatively easy to construct lattice-matched Co/Cr superlattices. For 4-layer superlattices, the advantage of using elements rather than compounds as constituents is marginal, but for the 6- and 8-layer superlattices discussed in detail in Sec. V, the advantage is already significant, while for the 10- to 14-layer systems considered briefly in Sec. VI, the advantage is overwhelming. However, as we will see shortly, the crystallographic simplicity of the Co/Cr system is counterbalanced by the fact that the antiferromagnetism of Cr is considerably more sensitive to physical conditions and computational details than is the antiferromagnetism of compounds such as MnFe.

II. THEORETICAL MODEL

Reduced to its essentials, our theoretical model is a crystallographically coherent F/AF superlattice composed of alternating ultrathin slabs of Co and Cr. Since these elements have nearly the same atomic volumes (within about 2%), it is reasonable to approximate this structure by a strained-layer superlattice, in which all atoms lie on a common lattice having suitably averaged dimensions. We will focus on Cr-rich superlattices having repeat periods ranging from 4 to 8 atomic layers, with [001] interfaces. Since the crystal structure of a strained-layer superlattice should be dictated by the majority constituent, we will assume that all Co and Cr atoms in our Cr-rich structures lie on a common bcc lattice. Although we regard these hypothetical superlattices primarily as theoretical models, we note that bcc Co overlayers have recently been grown on bcc Cr substrates,[12] suggesting that the laboratory synthesis of Co/Cr multilayers may also be feasible.

It is impractical to carry out first-principles calculations for spin-density wave (SDW) antiferromagnetic Cr because of the long wavelength (21 lattice spacings).[13] Moreover, SDW antiferromagnetism would most likely be suppressed in ultrathin Cr slabs. It is expedient to turn instead to the commensurate antiferromagnetic (*C*-AF) model,[14,15] according to which bcc Cr consists of two interpenetrating simple cubic lattices, with the atoms on the two lattices having opposite spin. Although *C*-AF-Cr provides only a rough approximation of SDW-AF-Cr, we can justify using the *C*-AF model for three reasons.

First, the calculations are greatly simplified. Even with the *C*-AF model, 8-layer superlattice studies require substantial computational effort. Second, the *C*-AF state of bulk Cr can be stabilized experimentally by the addition of certain transition metal impurities,[16] suggesting that ultrathin antiferromagnetic Cr slabs could be similarly stabilized. Third, the impurity-stabilized *C*-AF state of Cr is not likely to be suppressed by the $\sim 1\%$ reduction in lattice dimensions that Cr would suffer during the formation of Co/Cr strained-layer superlattices. In contrast, the SDW-AF state of bulk Cr is destroyed by even smaller reductions in lattice dimensions.[17]

III. COMPUTATIONAL METHOD

We determined the spin distributions in [001] bcc Co/Cr superlattices such as that shown in Fig. 1 by carrying out self-consistent spin-polarized electronic structure calculations using frozen cores, the first-principles LMTO method,[18,19] and the spin-density functional approximation of von Barth and Hedin.[20] The calculations were carried out using a modified version of the LMTO computer programs described in Ref. 19. Our version was redimensioned so that we could study systems containing as many as 18 atoms (per unit cell) using *s*, *p*, *d*, and *f* partial waves, and as many as 32 atoms using only *s*, *p*, and *d* partial waves. (All of this requires seven megabytes of storage on an IBM 3081. 1 byte$\equiv$8 binary digits.) The calculations included the so-called combined corrections; their neglect in comparison runs changed the calculated

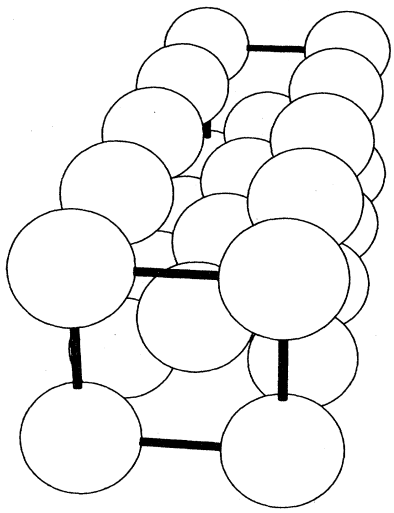

FIG. 1. Tetragonal unit cell for 8-layer [001] bcc superlattices. In Co(I)Cr(VII), for example, Co atoms lie on front and equivalent rear layers, while Cr atoms lie on intervening 7 layers. All atoms belonging to a given layer have the same spin.

spin moments by less than 1%. We checked some of our results by repeating selected calculations using LMTO programs developed by one of us (O.J.) based on a new orthogonalized LMTO formalism.[21]

To avoid possible confusion, we note at the outset that the electronic charge density of bcc C-AF-Cr has the same symmetry as the bcc lattice itself, while the spin density has a lower symmetry analogous to that of the cesium chloride structure, there being two atoms of opposite spin in the unit cell. For spin-polarized calculations, the unit cell of bcc C-AF-Cr is a cube in both direct and reciprocal space. A further point worth emphasizing is that our spin-density functionals are based on up and down spins, the directions of up and down not being keyed to the crystallographic axes in bulk crystals or to interfaces in superlattices. It is only after we include spin-orbit coupling and take magnetocrystalline anisotropy into account that we can say that the Co and Cr spins near an interface point parallel or perpendicular to that interface (or in some arbitrary direction). We emphasize that magnetocrystalline anisotropy is not taken into account in the present model.

In order to gain some experience with Co/Cr superlattices, we first carried out some preliminary calculations for bulk Co and Cr, and then examined several composite systems, always using the C-AF model for Cr. Contrary to earlier studies,[15] we found that sustained self-consistent iteration of C-AF-Cr leads to a paramagnetic rather than an antiferromagnetic state. The extremely slow convergence of antiferromagnetic calculations may have influenced some earlier workers to conclude that their solutions had converged to the C-AF state. We are presently developing improved LMTO computer programs which we intend to use to reexamine the question of the C-AF state of bulk Cr.

As an outgrowth of these studies, we developed a heuristic method for theoretically stabilizing the C-AF model of Cr.[22] Since this treatment appears to work quite well for composite systems such as Co/Cr superlattices, as well as for bulk Cr, we decided to base the present study entirely on this stabilized C-AF model, which we regard as the theoretical equivalent of the experimental impurity-stabilized C-AF state.[16]

IV. BULK COBALT AND CHROMIUM

Prior to treating composite Co/Cr systems, we studied the convergence of spin distributions in bulk Co and Cr as a function of the number of mesh points used in the three-dimensional integrations over the reduced zone. For materials having high symmetry and few atoms per unit cell, such as (bulk) hcp Co, bcc Co, and bcc Cr, it is necessary to use several hundred mesh points to obtain 1% accuracy, as can be seen from Table I. The computational effort required to carry out these integrations by the tetrahedron scheme[18,19,23] is proportional to I_K, the number of inequivalent points in the irreducible sector of the reduced zone. In Table I and in subsequent tables we show the total number of mesh points in the reduced zone as well as I_K, so that the reader can get a feeling for the size of each mesh as well as some idea of the computational effort involved.

As can be seen from Table I, the calculated spin moments μ_s for hcp and bcc Co gradually increase with increasing number of mesh points, eventually saturating. We know that μ_s(Co) depends on the difference between the densities of states for spin-up and spin-down electrons, DOS(+) and DOS(−). If only a small number of k points is sampled, the difference between DOS(+) and DOS(−) is determined only by the gross spectral structure of DOS(+) and DOS(−), and by the particular regions of the reduced zone that are sampled most accurately by the tetrahedron scheme. As I_K increases, the zone is sampled more uniformly, and larger differences can develop as the finer details of DOS(+) and DOS(−) are taken into account. This accounts for the rise in μ_s(Co) with increasing number of mesh points.

The dependence of μ_s(Co) and μ_s(Cr) on lattice constant is only slight, indicating that the Co and Cr moments for strained-layer superlattices should be nearly the same as for bulk samples. Comparing the spin moments for bcc Co having the same atomic volume as hcp Co, with the spin moment for hcp Co, we find that the spin moment for bcc Co is somewhat larger than that for hcp Co. This result is relevant to bcc Co overlayers grown on bcc Cr substrates.[12] Our results for bcc Co are consistent with other recent bulk bcc Co calculations based on a slightly different exchange-correlation potential.[24]

TABLE I. Convergence study: spin magnetic moments (in Bohr magnetons per atom) for bulk cobalt and chromium, for various meshes [calculated for equilibrium values of Wigner-Seitz sphere radii R(Co)=2.621 bohr and R(Cr)=2.684 bohr, except as otherwise noted]. Here and elsewhere, chromium is represented by the stabilized commensurate antiferromagnetic model (Ref. 22).

Total mesh points	12	144	324	960	2100	5292
Inequivalent points	8	27	48	125	252	576
Cobalt (hcp)	+1.312	+1.486	+1.528	+1.570	+1.579	+1.585
Cobalt (hcp)	+1.349[a]				+1.602[a]	
Total mesh points	8	64	216	512	8000	13 824
Inequivalent points	4	10	20	35	286	495
Cobalt (bcc)	+1.082	+1.344	+1.537	+1.625	+1.714	+1.717
Chromium (bcc)	±0.80	±0.54	±0.50	±0.50	±0.60	
Chromium (bcc)			±0.54[b]			

[a]Calculated for 1.01 R(Co).
[b]Calculated for 1.01 R(Cr).

TABLE II. Convergence study: spin magnetic moments for 4-layer bcc superlattices Co(IV), Cr(IV), and Co(I)Cr(III)=Co(1)Cr(2)Cr(3)Cr(4), for various meshes. For Co(I)Cr(III), atomic sites Cr(2) and Cr(4) are equivalent. Total number of mesh points in reduced zone is shown in parentheses.

Mesh for tetragonal reduced zone	Co(IV) (all-Co)	Cr(IV) (all-Cr)	Co(I)Cr(III) Co(1)	Cr(2)	Cr(3)	Cr(4)
$I_K=12$ (32)[a]	1.45		+0.90	+0.26	−0.19	+0.26
$I_K=20$ (72)[b]	1.56	±0.43	+1.37	+0.88	−0.44	+0.88
$I_K=30$ (128)	1.64	±0.34	+1.32	+0.85	−0.50	+0.85
$I_K=60$ (256)	1.71		+1.38	+0.99	−0.55	+0.99
$I_K=84$ (400)	1.72		+1.39	+1.00	−0.56	+1.00

[a]I_K is number of inequivalent mesh points in irreducible sector of reduced zone.
[b]This mesh is also used in following tables.

For bcc *C*-AF-Cr, we obtain nearly the same moment for all the meshes considered except the coarsest ($I_K=4$), which places undue emphasis on nonrepresentative high-symmetry points in the reduced zone. For the remaining meshes, the near uniformity of the calculated Cr moments is due primarily to the theoretical stabilization of the *C*-AF-Cr model.

V. STRAINED-LAYER COBALT/CHROMIUM SUPERLATTICES

Because of the lower (tetragonal) symmetry of our superlattices, and the larger number of atoms per unit cell, achieving 1% accuracy in spin-moment calculations would require enormous computational effort. Accordingly, we had to reach a compromise between accuracy and computer time. Based on the convergence study for 4-layer superlattices shown in Table II, and on similar studies for other superlattices, we concluded that a 72-point mesh was adequate for our purposes. In order to be able to compare the magnitudes of Co and Cr spin moments in superlattices with their corresponding bulk values—at the same level of convergence—we also studied all-Co and all-Cr 4-, 6-, and 8-layer bcc superlattices (cf. Tables II through V).

If we use sufficiently fine meshes for the all-Co and all-Cr bcc superlattices, we should obtain the same results as those given by the bulk bcc-Co and Cr calculations, apart from minor differences in lattice constants. As can be seen by comparing the results in Tables II–V with those in Table I, we do not obtain identical results because of incomplete convergence of the superlattice calculations. Nevertheless, if we make allowance for the different meshes used for bulk Co and Cr on the one hand, and the all-Co and all-Cr superlattices on the other hand, all the results in these tables prove mutually consistent.

We investigated the following structures:

(i) 4-layer superlattices—Co(I)Cr(III), Co(IV), and Cr(IV),

(ii) 6-layer superlattices—Co(I)Cr(V), Co(VI), and Cr(VI),

(iii) 8-layer superlattices—Co(I)Cr(VII), Co(III)Cr(V), Co(VIII), and Cr(VIII).

Roman numerals denote the number of successive Co or Cr atoms in the repeat period. For example, the repeat period of Co(I)Cr(III) is Co(1)Cr(2)Cr(3)Cr(4), where the arabic numerals identify the atomic site or layer. We started off our calculations for these Co/Cr superlattices using a variety of assumed spin distributions, and then iterated to self-consistency. We also tried different starting distributions to see whether we could generate alternate self-consistent solutions. The only restraint we imposed was that all atoms in the same atomic layer have the same spin moment, as would be expected for [001] interfaces and the *C*-AF model for Cr. The magnetic properties of all the composite superlattices were dominated by the ferromagnetic Co layers.

For the Co/Cr superlattices containing only one Co layer, namely, Co(I)Cr(III), Co(I)Cr(V), and Co(I)Cr(VII), there is only one self-consistent spin distribution, and this has the following key features.

(i) Spin moments of the interfacial Cr atoms are aligned parallel to the spin moments of the Co atoms (ferromagnetic coupling across the interfaces).

(ii) Spin moments of the Cr atoms alternate from layer to layer (antiferromagnetic arrangement).

(iii) Spin moments of the Co atoms are reduced and the spin moments of the interfacial Cr atoms are enhanced relative to their bulk values.

Generalizing these results, we anticipate that the interfa-

TABLE III. Spin magnetic moments for bcc superlattices Co(VI), Cr(VI), and Co(I)Cr(V)=Co(1)Cr(2)Cr(3)Cr(4)Cr(5)Cr(6). Atomic sites in same column are equivalent.

Mesh for tetragonal reduced zone	Co(V) (all sites cobalt)	Cr(VI) (all sites chromium)	Co(I)Cr(V) Co(1)	Cr(2) Cr(6)	Cr(3) Cr(5)	Cr(4)
$I_K=20$ (72)[a]	1.65	±0.38	+1.46	+0.94	−0.42	+0.36

[a]Parentheses as in Table II.

TABLE IV. Spin magnetic moments for 8-layer bcc superlattices Cr(VIII) and Co(I)Cr(VII)=Co(1)Cr(2)···Cr(8). Atomic sites in same column are equivalent.

Mesh for tetragonal reduced zone	Cr(VIII) (all sites chromium)	Co(I)Cr(VII) Co(1)	Cr(2) Cr(8)	Cr(3) Cr(7)	Cr(4) Cr(6)	Cr(5)
$I_K=20$ (72)[a]	±0.53	+1.35	+0.97	−0.41	+0.36	−0.33

[a]Parentheses as in Table II.

cial coupling will always be ferromagnetic for Co/Cr superlattices having single Co layers separated by multiple Cr layers. In the simplest cases, successive Co layers will have parallel or antiparallel spins accordingly as the number of intervening Cr layers is odd or even. More complicated spatially modulated spin distributions can also be visualized.

For Co(III)Cr(V), which contains 3 adjacent Co layers separated by 5 adjacent Cr layers, the essential results are as follows:

(i) There are two distinct spin distributions, corresponding to parallel and antiparallel alignments of the interfacial Co and Cr spins (ferromagnetic as well as antiferromagnetic interfacial coupling).

(ii) For both cases, the Cr regions are antiferromagnetic (*C*-AF model).

(iii) For both cases, all Co and Cr spin moments are reduced relative to their respective bulk values; moreover, the Co moments for the interfacial layers are smaller than the moments of the central Co layer.

Since there was only one spin distribution for Co(I)Cr(V), which also contains 5 adjacent Cr layers, we attribute the added degree of freedom in Co(III)Cr(V) to the presence of more than 1 adjacent Co layer. The added flexibility arises from the possibility of moment redistribution in the interfacial and central Co layers. We would expect analogous results for still thicker Co slabs.

The general features just found for [001] Co/Cr superlattices should also apply to [111] Co/Cr superlattices, because all atoms in interfacial Cr layers have the same spin for both of these orientations (*C*-AF model). On the other hand, for [110] Co/Cr superlattices, the interfacial Cr layers would be compensation planes (equal numbers of up and down spins). Since our calculations indicate that only ferromagnetic coupling is supported across single-layer Co interfaces, we would expect the *C*-AF state of Cr to be suppressed near [110] single-layer Co interfaces. By the same token, we would expect the *C*-AF state as well as more complicated antiferromagnetic spin orderings of Cr to be sustained near [110] multiple-layer Co interfaces.

On the basis of the above results, including the similarity of the spin moments in bcc Co and hcp Co, we can make certain predictions concerning the spin distributions in Co-rich hcp Co/Cr strained-layer superlattices. These structures are the counterparts of the Cr-rich bcc Co/Cr strained-layer superlattices considered above. In Co-rich variety, we would expect all the atoms to lie on a common lattice (hcp) determined by the majority constituent (Co). Since the hcp lattice consists of two interpenetrating primitive hexagonal lattices, we could again visualize a commensurate antiferromagnetic spin arrangement for the Cr atoms: There would be opposite spins on the two sets of Cr atoms belonging to the two primitive hexagonal lattices. We would again expect ferromagnetic coupling at single-layer Co interfaces, and both ferromagnetic and antiferromagnetic coupling at multiple-layer Co interfaces. More complicated Co/Cr superlattices are discussed briefly in the next section

VI. LATTICE-MATCHED hcp-Co/bcc-Cr SUPERLATTICES

Strained-layer Co/Cr superlattices all of whose atoms lie on a common lattice represent a special class of lattice-matched composite structures. A more general class can be formed from alternating slabs of Co and Cr having different crystal structures but so oriented that there is exact (or nearly exact registry) at the interfaces.

The most striking example[25] is the lattice-matched interface between the [210] plane of hcp Co shown in Fig. 2 and the [112] plane of bcc Cr shown in Fig. 3. For bulk Co, the dimensions of the primitive interface rectangle in Fig. 2 are $a(\mathrm{Co})=2.5071$ Å and $c(\mathrm{Co})=4.0686$ Å. For bulk Cr, the corresponding dimensions for the matching rectangle in Fig. 3 are $a^*(\mathrm{Cr})=\sqrt{3}a(\mathrm{Cr})/2=2.4975$ Å, and $c^*(\mathrm{Cr})=\sqrt{2}a(\mathrm{Cr})=4.0785$ Å, where $a(\mathrm{Cr})$ is the Cr unit cube edge. The closeness of the match between the

TABLE V. Spin magnetic moments for 8-layer bcc superlattices Co(VIII) and Co(III)Cr(V)=Co(1)Co(2)Co(3)Cr(4)···Cr(8). Atomic sites in same column are equivalent. Note two distinct solutions.

Mesh for tetragonal reduced zone	Co(VIII) (all sites cobalt)	Co(III)Cr(V) Co(1)	Co(2) Co(8)	Cr(3) Cr(7)	Cr(4) Cr(6)	Cr(5)
$I_K=20$ (72)[a]	+1.72	+1.52	+1.28	−0.29	+0.22	−0.11
$I_K=20$ (72)	+1.72	+1.53	+1.38	+0.16	−0.22	+0.47

[a]Parentheses as in Table II.

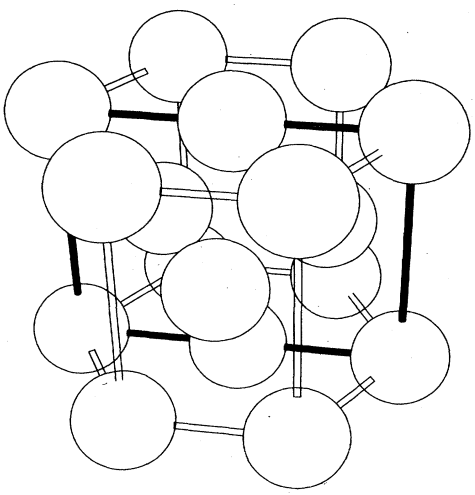

FIG. 2. Hexagonal close-packed structure, with [210] interface indicated by heavy lines.

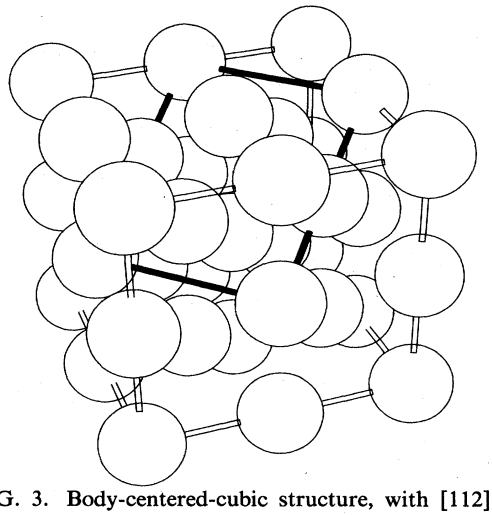

FIG. 3. Body-centered-cubic structure, with [112] interface indicated by heavy lines. For the Co/Cr system, this interface matches the [210] hcp interface shown in Fig. 2.

hcp-Co and bcc-Cr rectangles is perhaps best appreciated by expressing the dimensions as $a(\mathrm{Co/Cr})=2.5023 \pm 0.0048$ Å, and $c(\mathrm{Cr/Co})=4.0736 \pm 0.0050$ Å. For the C-AF state of Cr, the [112] interface is a compensation plane composed of alternating rows of down and up Cr spins.

Another example involves matching the [100] plane of hcp Co shown in Fig. 4 and the 45°-rotated [001] plane of bcc Cr shown in Fig. 5. For bulk hcp Co, the primitive [100] rectangle is nearly a square, having dimensions 4.0686 and 4.3424 Å. This nearly matches the heavy-line square shown in Fig. 5, whose edge for bulk bcc Cr is 4.0785 Å. The match is almost exact in one dimension, and off by about 6% in the other. For this geometry, all Cr atoms lying in a plane parallel to the interface would have the same spin.

Before discussing interfaces between hcp Co and bcc Cr, however, let us examine the simpler case of [112] strained-layer bcc superlattices having 1 Co layer per repeat period. If the number of atoms in the repeat period is a multiple of 6, the unit cell is orthorhombic, otherwise it is monoclinic. It is impractical to study monoclinic lattices because of their low symmetry. Accordingly, we consider the smallest orthorhombic structure, Co(I)Cr(V), which contains 6 layers per repeat period (cf. Fig. 6). Even though the orthorhombic structure is more symmetric than the monoclinic, it is less symmetric than the tetragonal structure (cf. Sec. V). Because the [112] interface is a compensation plane, we must use 2 atoms per layer to allow for the opposite Cr spins. With 12 atoms per repeat period (2 Co and 10 Cr), and orthorhombic symmetry, the computational effort is considerably

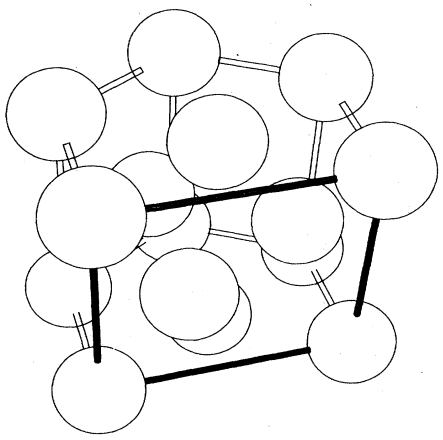

FIG. 4. Hexagonal close-packed structure, with [100] interface indicated by heavy lines.

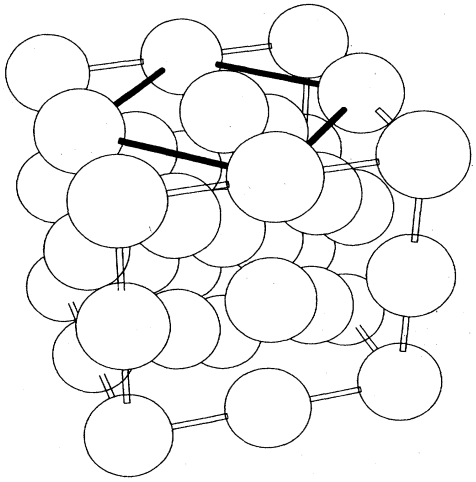

FIG. 5. Body-centered-cubic structure, with 45°-rotated [001] interface indicated by heavy lines. For the Co/Cr system, this interface matches the [100] hcp interface shown in Fig. 4.

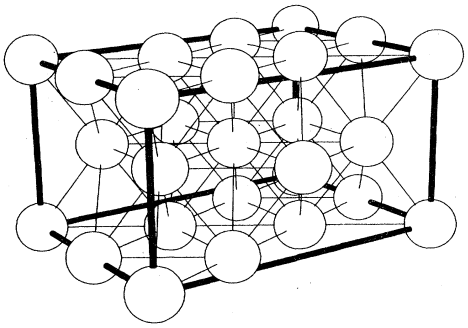

FIG. 6. Orthorhombic unit cell for 6-layer [112] bcc superlattices. In Co(I)Cr(V), for example, Co atoms lie on front and equivalent rear layers, and Cr atoms on intervening 5 layers.

greater than for 8-layer tetragonal structures.

Preliminary calculations for this 12-atom orthorhombic structure yield only one solution corresponding to ferromagnetic coupling across the single Co-layer interface, confirming our earlier results for single Co-layer [001] superlattices. The spin ordering in the Cr region remains antiferromagnetic, but the spin moments are reduced considerably by the restraint imposed by the single Co-layer interface.

We can now construct [210] hcp-Co/[112] bcc-Cr superlattices by introducing additional layers which have the hcp rather than the bcc stacking, as illustrated in Figs. 7 and 8. In order to maintain an orthorhombic unit cell, the number of sequential layers having the hcp structure must be a multiple of 4. The simplest lattice-matched [210] hcp-Co/[112] bcc-Cr superlattice having an orthorhombic unit cell is therefore the 10-layer structure shown in Fig. 7. The superlattice stoichiometry depends on the occupancy of the two inequivalent frontier layers. In Co(V)Cr(V), Co(IV),Cr(VI), and Co(III)Cr(VII), Cr atoms lie on neither, either, or both frontier layers, respectively. The next largest orthorhombic superlattice of this type is the 14-layer structure shown in Fig. 8. This contains one bcc cycle (6 layers) and two hcp cycles (8 layers). For Co(IX)Cr(V), Co(VIII)Cr(VI), and Co(VII)Cr(VII), Cr atoms lie on neither, either, or both frontier layers, respectively. The next largest superlattice would be a 16-layer structure containing two bcc cycles (12 layers) and one hcp cycle (4 layers), etc.

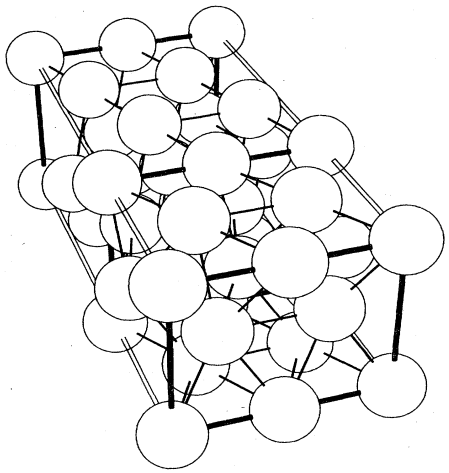

FIG. 7. Orthorhombic unit cell for 10-layer [210] hcp-Co/[112] bcc-Cr superlattices. Frontier layers common to hcp and bcc regions are indicated by heavy lines. The hcp region is in front.

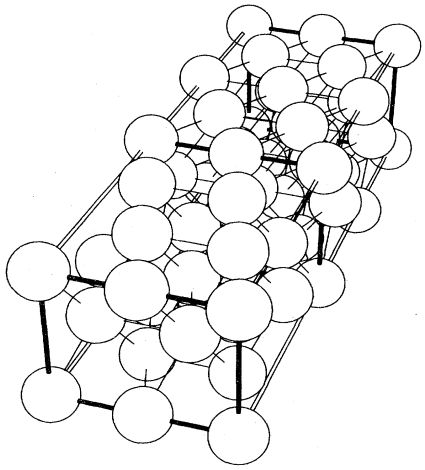

FIG. 8. Orthorhombic unit cell for 14-layer [210] hcp-Co/[112] bcc-Cr superlattices. Frontier layers common to hcp and bcc regions are indicated by heavy lines. Here the bcc region is in front.

We have investigated the electronic and magnetic structure of a number of these superlattices, but we will confine ourselves here to the prototype, the 10-layer Co(III)Cr(VII) structure. In order to simplify the calculations, we first assumed that all atoms in the same layer have the same spin, so that the repeat period contains only 10 atoms (3 Co and 7 Cr). We found that the Co spin moments are larger for the central Co layer than for the interfacial Co layers, that the interfacial Cr layers are weakly magnetized, and that the remaining Cr layers are hardly magnetized at all. We then allowed alternating rows in each Cr layer to have opposite spin, and alternating rows in each Co layer to have different spin moments of the same sign. Since there are now 2 inequivalent atoms per layer, the unit cell contains 20 atoms, making the calculations rather costly. Since we could only use a limited number of mesh points, our results are suggestive rather than conclusive, but in general we found that the Cr regions became more strongly magnetized than before, the spin arrangement being antiferromagnetic. This is consistent with our earlier prediction that multiple-layer Co slabs can support antiferromagnetic spin arrangements in adjacent Cr slabs.

Finally, we turned to the [100] hcp-Co/[001] bcc-Cr superlattices (cf. Figs. 4 and 5), which are closely matched in one direction and mismatched by about 6% in the other. Since we are not in a position to relieve the strain by introducing misfit dislocations, we again turned to the idea of strained-layer superlattices, concentrating on the Co(III)Cr(V) structure, which is very similar to the [001]

Co(III)Cr(V) strained-layer bcc superlattice studied earlier, except for the different spacings in the Co region, and the slightly distorted unit cell, which is now orthorhombic rather than tetragonal. We decided to ignore the 3% deviations from tetragonality, which we judged to be of minor importance. Using a tetragonal unit cell, we obtained substantially the same results as before, indicating that the detailed atomic arrangements in the Co region are of minor importance so far as the exchange coupling across the interface is concerned. Thus, our results for the [001] strained-layer bcc Co/Cr superlattices apply to more general interface geometries as well.

VII. CONCLUDING REMARKS

To recapitulate, we have calculated the exchange coupling and spin distributions in ferromagnetic/antiferromagnetic strained-layer superlattices composed of ultrathin Co and Cr slabs. By calling attention to these hypothetical superlattices, we hope to stimulate interest in the laboratory synthesis of such artificially layered structures. We also hope that our work will stimulate further theoretical studies of the impurity-stabilized commensurate antiferromagnetic state of Cr, and of the spin-density-wave antiferromagnetic state of Cr.[26] We are currently exploring the possibility of incorporating magnetocrystalline anisotropy into the present theoretical model, with a view to carrying out first-principles investigations of exchange anisotropy.

ACKNOWLEDGMENTS

We are particularly grateful to H. L. Skriver for sending us a copy of his LMTO computer programs in advance of publication, and for fruitful discussions. We have also benefited from stimulating discussions with our colleagues, O. K. Andersen, J. Kent Howard, R. H. Geiss, K. Lee, N. H. March, R. K. Nesbet, S. S. P. Parkin, and C. Schlenker. One of us (P.L.) wishes to thank IBM Belgium for making it possible for him to spend a year at IBM San Jose Research Laboratory. We are also grateful to the U. S. Office of Naval Research for partial support.

---

*On leave from Facultés Universitaires, Notre Dame de la Paix, Namur, Belgium.

[1]A. J. Forty, Contemp. Phys. **24**, 271 (1983); G. E. Rhead, *ibid.* **24**, 535 (1983), and references cited.

[2]*Synthetic Structurally Modulated Materials,* edited by L. L. Chang and B. C. Giessen (Academic, New York, in press).

[3]Semiconductors: G. H. Dohler, Sci. Amer. **249**, 144 (1983); F. J. Grunthaner and A. Madhukar, J. Vac. Sci. Technol. **B1**, 462 (1983); F. Herman, J. Phys. (Paris) Colloq. **45**, C5-375 (1984). Metallic systems: C. M. Falco and I. K. Schuller, in *Novel Materials and Techniques in Condensed Matter,* edited by G. W. Crabtree and P. Vashishta (North-Holland, New York, 1982); C. M. Falco, J. Phys. (Paris) Colloq. **45**, C5-499 (1984).

[4]G. Bergmann, Phys. Rev. Lett. **41**, 264 (1979); G. Bergmann, Phys. Today **32**(8), 25 (1979); C. Rau, Comments Solid State Phys. **9**, 177 (1980); R. Meservey, P. M. Tedrow, and V. R. Kalvey, Solid State Commun. **36**, 969 (1980); C. Rau and S. Eichner, Phys. Rev. Lett. **47**, 939 (1981); I. Kramer and G. Bergmann, Phys. Rev. B **27**, 7271 (1983); R. H. Victora and L. M. Falicov, *ibid.* **28**, 5232 (1984); J. S. Moodera and R. Meservey, *ibid.* **29**, 2943 (1984); S. Ohnishi, M. Weinert, and A. J. Freeman, *ibid.* **30**, 36 (1984); R. H. Victora and L. M. Falicov, *ibid.* **28**, 5232 (1983); R. H. Victora, L. M. Falicov, and S. Ishida, *ibid.* **30**, 3896 (1984); L. M. Falicov, R. H. Victora, and J. Tersoff (unpublished).

[5]W. M. C. Yang, T. Tsakalakos, and J. E. Hilliard, J. Appl. Phys. **48**, 876 (1977); E. M. Gyorgy, J. F. Dillon, Jr., D. B. McWham, L. W. Rupp, Jr., L. R. Testardi, and P. J. Flanders, Phys. Rev. Lett. **45**, 57 (1980); T. Jarlborg and A. J. Freeman, *ibid.* **45**, 653 (1980); J. Appl. Phys. **53**, 8041 (1982); A. J. Freeman, J. Magn. Magn. Mater. **35**, 31 (1983); T. Shinjo, N. Hosoito, K.Kawaguchi, T. Takada, Y. Endoh, Y. Ajiro, and J. M. Friedt, J. Phys. Soc. Jpn. **52**, 3154 (1983); Y. Isshiki, T. Kambara, and K. I. Gondaira, J. Magn. Magn. Mater. **35**, 11 (1983); N. Hamada, K. Terakura, and A. Yanase, *ibid.* **35**, 7 (1983); M. R. Khan, Phys. Rev. B **27**, 7186 (1983).

[6]R. M. White and D. J. Friedman (unpublished).

[7]W. H. Meiklejohn, J. Appl. Phys. **33**, 1328 (1962); A. Yelon, Phys. Thin Films **6**, 205 (1971).

[8]B. D. Cullity, *Introduction to Magnetic Materials,* (Addison-Wesley, Reading, Mass., 1972); N. H. March, P. Lambin, and F. Herman, J. Magn. Magn. Mater. **44**, 1 (1984).

[9]R. D. Hempstead, S. Krongelb, and D. A. Thompson, IEEE Trans. Magn. **MAG-14**, 521 (1978).

[10]J. Kent Howard (private communication).

[11]P. Lambin and F. Herman, Phys. Rev. B **30**, 6903 (1984).

[12]R. Walmsley, J. Thomson, D. Friedman, R. M. White, and T. H. Geballe, IEEE Trans. Magn. **MAG-19**, 1992 (1983).

[13]W. M. Lomer, Proc. Phys. Soc. **80**, 489 (1962); G. Shirane and W. Takei, J. Phys. Soc. Jpn. Suppl. **17BIII**, 35 (1962); G. C. Windsor, J. Phys. F **2**, 742 (1972); T. Ukai and N. Mori, J. Appl. Phys. **53**, 2038 (1982).

[14]A. C. Switendick, J. Appl. Phys. **37**, 1022 (1966); S. Asano and J. Yamashita, J. Phys. Soc. Jpn. **23**, 714 (1969); **31**, 1000 (1971); Prog. Theor. Phys. **49**, 373 (1973). These authors either failed to obtain the antiferromagnetic state of Cr or obtained it using unphysical exchange-correlation potentials.

[15]H. L. Skriver, J. Phys. F **11**, 97 (1981); J. Kubler, J. Magn. Magn. Mater. **20**, 277 (1980), and references cited.

[16]W. C. Koehler, R. M. Moon, A. L. Trago, and A. R. Mackintosh, Phys. Rev. **151**, 405 (1966); Y. Endoh, Y. Ishikawa, and H. Ohno, J. Phys. Soc. Jpn. **24**, 263 (1968).

[17]D. B. McWhan and T. M. Rice, Phys. Rev. Lett. **19**, 846 (1967); P. C. Pattnaik, P. H. Dickinson, and J. L. Fry, Phys. Rev. B **28**, 5281 (1983).

[18]O. K. Andersen, Phys. Rev. B **12**, 3060 (1975); O. Jepsen, O. K. Andersen, and A. R. Mackintosh, *ibid.* **12**, 3084 (1975); O. K. Anderson and O. Jepsen, Physica **91B**, 317 (1977).

[19]H. L. Skriver, *The LMTO Method* (Springer, Berlin, 1984).

[20]U. von Barth and L. Hedin, J. Phys. C **5**, 1629 (1972).

[21]O. K. Andersen, O. Jepsen, and D. Glotzel, in *Highlights of Condensed Matter Theory, proceedings of the International*

School of Physics, Enrico Fermi, Varenna, July 1983 (Plenum, New York, 1984).
[22]F. Herman and H. L. Skriver (unpublished).
[23]O. Jepsen and O. K. Andersen, Solid State Commun. **9**, 1763 (1971).
[24]D. Bagayoko, A. Ziegler, and J. Callaway, Phys. Rev. B **27**, 7046 (1983).
[25]J. Daval and D. Randet, IEEE Trans. Magn. **MAG-6**, 768 (1970).
[26]A. W. Overhauser, Phys. Rev. **128**, 1437 (1962); P. A. Fedders and P. C. Martin, *ibid.* **143**, 245 (1966); L. M. Falicov and D. R. Penn, *ibid.* **158**, 476 (1967); and references cited.